# ASCE/SEI 41 PREDICTED PERFORMANCE OF NEWLY DESIGNED BRBFS

## M.S. Speicher[1], J.L. Harris[2]

[1] *Research Structural Engineer, National Institute of Standards and Technology, matthew.speicher@nist.gov*
[2] *Research Structural Engineer, National Institute of Standards and Technology, john.harris@nist.gov*

## Abstract

Structural engineers in the United States have turned to performance-based design methodologies for design of new buildings in order to find improved design solutions as compared to those obtained using prescriptive design provisions of current model building codes or standards, such as ASCE/SEI 7. Performance-based seismic design of existing buildings has been implemented in the U.S. for seismic retrofits during the past decade (e.g., ASCE/SEI 41). Engineers are now starting to rely more heavily on the existing building procedures in ASCE/SEI 41 for the design of new buildings in order to obtain satisfactory seismic performance in the most cost effective manner. However, a translation between the two approaches is not direct and can often be a challenge due to perceived conservatism in the ASCE/SEI 41 procedures and the disjointed seismic performance expectations between ASCE/SEI 7 and ASCE/SEI 41. This paper presents the results of a performance assessment of six newly designed buckling-restrained braced frames to examine the correlation between ASCE/SEI 7 and ASCE/SEI 41. Two buildings are designed at each of the following heights: 4, 8, and 16 stories—one using the equivalent lateral force procedure and the other using the response spectrum analysis procedure. The performance of the buckling-restrained brace components is then assessed using the linear static, linear dynamic, nonlinear static, and nonlinear dynamic procedures in ASCE/SEI 41. The linear and nonlinear results generally indicate acceptable performance (except for the 8-story frames) which gives insight into how ASCE/SEI 7 and ASCE/SEI 41 compare. Additionally, the linear results are not always more conservative than the nonlinear results, which is counterintuitive and is discussed in the context of the results.

*Keywords: buckling-restrained braced frames; steel structures; performance-based seismic design; seismic retrofit*

## 1. Introduction

Prescriptive building code procedures, such as those found in the International Building Code [1] and ASCE/SEI 7 (hereafter ASCE 7) [2], may restrict design innovation, leading to potentially inefficient structural designs and higher construction costs. However, ASCE 7 allows alternative rational design methods to be used in lieu of its prescriptive provisions but provides no substantial guidance on implementing these methods. Therefore, many practitioners have turned to ASCE/SEI 41 (hereafter ASCE 41) [3], the standard for seismic assessment of existing buildings, to implement "first-generation" performance-based seismic design (PBSD) principles for the design of new buildings.

This paper presents select results from a study investigating the correlation between the intended seismic performance of an ASCE 7 code-compliant building and its performance as quantified using ASCE 41 procedures. This investigation is performed by evaluating the seismic performance of six buckling-restrained braced frame (BRBF) steel buildings designed for a region of high seismicity. The basic question is whether the standards for designing new steel buildings and assessing existing steel buildings provide consistent levels of performance. In this paper, the performance of the buckling-restrained braced (BRB) components is assessed using the linear static, linear dynamic, nonlinear static, and nonlinear dynamic procedures in ASCE 41. First, the archetype buildings will be presented. This is followed by the seismic performance assessment and associated discussions. This study is a follow-on to previous work on special concentrically braced frames [4, 5], eccentrically braced frames [6, 7], and special moment frames [8].

## 2. Archetype Building Design

A set of six office buildings is designed for this study. The building heights investigated are 4, 8, and 16 stories. The building framing layout is symmetric with five 9.1 m bays in the E-W direction and five 6.1 m bays in the N-S direction. The first story height is 5.5 m and the remaining story heights are 4.3 m. The seismic force-resisting system (SFRS) is composed of perimeter special moment frames (SMF) in the E-W direction and perimeter BRBFs in the N-S direction. Only the performance of the BRBFs in the N-S direction are investigated in this paper. The BRBs are placed in an inverted-V configuration in the 4-story frame and in a two-story X configuration in the 8- and 16-story frames. Additionally, the 16-story frames have the two braced bays placed adjacent to each other, as is indicated in the building plan view in Fig. 1.

The building is designed for all load effects in accordance with ASCE 7-10, AISC 360-10 [9], and AISC 341-10 [10]. Each building is assumed to be located in a region of high seismicity and is assigned to Seismic Design Category D with spectral accelerations at 0.2 s. ($S_S$) and 1.0 s. ($S_1$) of 1.5 g and 0.6 g, respectively. Two buildings are designed at each height, using seismic effects computed by either the equivalent lateral force (ELF) procedure or the response spectrum analysis (RSA) procedure. Though the ELF procedure is not allowed for the 16-story frame due to height limitations in ASCE 7, this limitation is ignored in this study. For the RSA-designed frames, the total modal base shear is scaled to 85 % of that computed using the ELF. Accidental eccentricity is included and orthogonality effects are considered. The redundancy factor, $\rho$, is 1.0. Effective seismic weights are set as dead load plus 20 % of the unreduced floor live load to represent partition weight (0.48 kN/m$^2$). For drift analysis (including period calculation) and stability verification, the story gravity load is set as dead load plus 25 % of the unreduced floor live load.

Floor and roof dead load consists of steel and slab weight (82 mm lightweight concrete (1760 kg/m$^3$) on 75 mm metal deck ≈ 2.2 kN/m$^2$). Superimposed dead load is 0.72 kN/m$^2$ for floors and 0.48 kN/m$^2$ for the roof, and includes mechanical, electrical, plumbing and other miscellaneous items. A 3.3 kN/m superimposed dead load is applied to the perimeter framing for façade weight (curtain wall). The edge of slab is 0.3 m from perimeter framing. Live load is 2.4 kN/m$^2$ for floors and 1.5 kN/m$^2$ for the roof.

The wind speed is 177 km/h and 116 km/h for the 700-year (design) and 10-year wind (drift), respectively. The structure is assigned Exposure B and not considered rigid. The gust factors (assuming 2 % damping) are 1.10 for the 700-year wind and 0.94 for the 10-year wind. Torsional wind effects are considered, and the

directionality factor, $k_d$, is 0.85. Wind effects do not control member sizes except for the bottom two stories of the 16-story frame.

The building is considered fixed at the seismic base. The base columns of the SFRS are embedded into a foundation wall. As such, column bases are modeled as fixed in the plane of the frame and pinned out-of-plane. Non-SFRS gravity column bases are considered pinned in both orthogonal directions. Strength and drift checks are done with a conventional second-order elastic analysis (i.e., constant stiffness matrix), and do not account for material nonlinearity or geometric imperfections (except for gravity-only load combinations). Drift limits are $h$/50 (amplified) for seismic and $h$/400 (elastic) for wind (10-year), where $h$ is the story height. Composite action with the slab is not considered for checking seismic drifts but is included for checking wind drifts. For all the frames, the BRB, beam, and column member sizes and accompanying BRB stiffness modification factor, *KF*, are listed in Table 1. *KF* is used to adjust the axial stiffness of the steel core alone to that of the actual component.

The mathematical model is based on centerline dimensions with rigid-end offsets at the beam-to-column joints. The buildings are modeled in three dimensions in ETABS [11]. In the BRBFs, the beam ends are fixed to the columns to account for gusset plate restraint. The added stiffness caused by the gusset plate is approximated by doubling the adjacent member stiffnesses over an estimated plate length of 0.46 m (18 in.). At the end of the gusset plate, the beam is spliced with a shear tab connection, which is idealized as pinned. The brace is also assumed to be pinned at the ends, thus it only carries axial load. The brace member is assigned an area equal to the BRB steel core area and spans between work points (w.p.). Since the actual stiffness of the BRB is higher than $A_{sc} \times E / L_{w.p.}$ due to the stiffened portion outside the reduced core and the accompanying connection zone (i.e., gusset plate, member depths, etc.), a stiffness modifier, *KF*, is applied. These values are typically provided by the brace manufacturer. In this study, an average value from those received by several manufactures was used.

The floor slabs are modeled as semi-rigid membrane diaphragms with no out-of-plane bending stiffness and a 0.5 in-plane stiffness modifier to account for cracking at design loads. Gravity load-carrying framing is modeled to capture *P*-Δ effects. The gravity beams are assumed to be pinned at the ends to minimize their strength and stiffness contribution to the seismic performance of the BRBFs. Steel properties are those for A992 for beams and columns ($F_y$ = 345 MPa and $R_y$ = 1.1). The BRB core material is assumed to have an $F_y$ = 317 MPa.
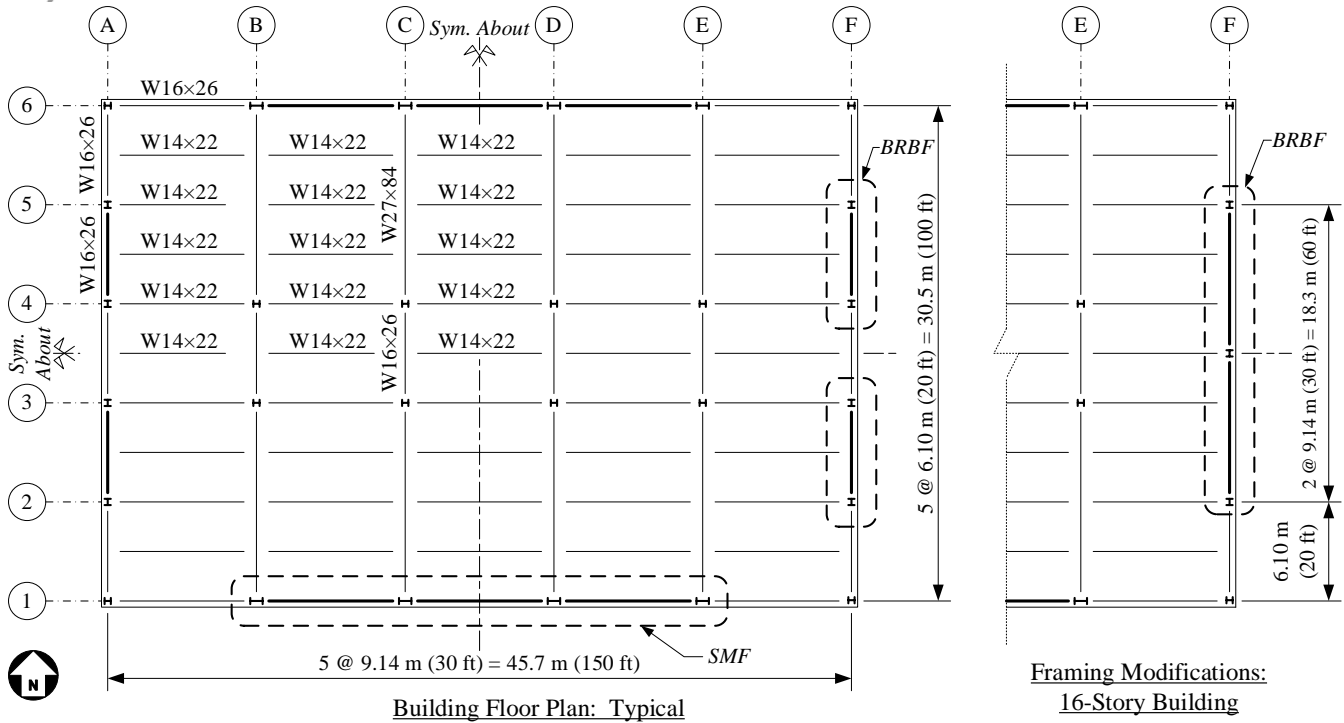
Fig. 1 – Building plan view for all designs used in this study

Table 1 – Member sizes for the BRBFs

| | | ELF designs | | | | | | RSA designs | | | |
|---|---|---|---|---|---|---|---|---|---|---|---|
| | story | brace $A_{sc}^{(1)}$ (cm$^2$) | KF | beam | column | | story | brace $A_{sc}^{(1)}$ (cm$^2$) | KF | beam | column |
| 4-story | 4 | 8.06 | 1.46 | W16×31 | W14×48 | 4-story | 4 | 6.45 | 1.45 | W16×31 | W14×48 |
| | 3 | 12.9 | 1.46 | W16×31 | W14×48 | | 3 | 11.3 | 1.45 | W16×31 | W14×48 |
| | 2 | 19.4 | 1.46 | W16×31 | W14×82 | | 2 | 16.1 | 1.45 | W16×31 | W14×74 |
| | 1 | 22.6 | 1.46 | W16×31 | W14×82 | | 1 | 17.7 | 1.45 | W16×31 | W14×74 |
| 8-story | 8 | 6.45 | 1.50 | W18×46 | W14×38 | 8-story | 8 | 6.5 | 1.48 | W18×46 | W14×38 |
| | 7 | 11.6 | 1.50 | W16×31 | W14×38 | | 7 | 11.3 | 1.48 | W16×31 | W14×38 |
| | 6 | 16.1 | 1.50 | W18×46 | W14×68 | | 6 | 11.3 | 1.48 | W18×46 | W14×68 |
| | 5 | 21.0 | 1.50 | W16×31 | W14×68 | | 5 | 12.9 | 1.48 | W16×31 | W14×68 |
| | 4 | 21.0 | 1.50 | W18×46 | W14×132 | | 4 | 14.5 | 1.48 | W18×46 | W14×82 |
| | 3 | 25.8 | 1.50 | W16×31 | W14×132 | | 3 | 17.7 | 1.48 | W16×31 | W14×82 |
| | 2 | 25.8 | 1.50 | W18×46 | W14×145 | | 2 | 19.4 | 1.48 | W18×46 | W14×132 |
| | 1 | 29.0 | 1.50 | W18×60 | W14×145 | | 1 | 24.2 | 1.48 | W18×60 | W14×132 |
| 16-story | 16 | 6.45 | 1.42 | W18×55 | W14×48 | 16-story | 16 | 6.45 | 1.41 | W18×55 | W14×48 |
| | 15 | 11.3 | 1.42 | W16×45 | W14×48 | | 15 | 11.3 | 1.41 | W16×45 | W14×48 |
| | 14 | 16.1 | 1.42 | W18×55 | W14×68 | | 14 | 14.5 | 1.41 | W18×55 | W14×68 |
| | 13 | 21.0 | 1.42 | W16×45 | W14×68 | | 13 | 16.1 | 1.41 | W16×45 | W14×68 |
| | 12 | 24.2 | 1.42 | W18×55 | W14×132 | | 12 | 17.7 | 1.41 | W18×55 | W14×132 |
| | 11 | 27.4 | 1.42 | W16×45 | W14×132 | | 11 | 19.4 | 1.41 | W16×45 | W14×132 |
| | 10 | 30.6 | 1.42 | W18×55 | W14×145 | | 10 | 19.4 | 1.41 | W18×55 | W14×132 |
| | 9 | 33.9 | 1.42 | W16×45 | W14×145 | | 9 | 24.2 | 1.41 | W16×45 | W14×132 |
| | 8 | 35.5 | 1.42 | W18×55 | W14×211 | | 8 | 27.4 | 1.41 | W18×55 | W14×176 |
| | 7 | 38.7 | 1.42 | W16×45 | W14×211 | | 7 | 29.0 | 1.41 | W16×45 | W14×176 |
| | 6 | 38.7 | 1.42 | W18×55 | W14×283 | | 6 | 32.3 | 1.41 | W18×55 | W14×233 |
| | 5 | 40.3 | 1.42 | W16×45 | W14×283 | | 5 | 33.9 | 1.41 | W16×45 | W14×233 |
| | 4 | 40.3 | 1.42 | W18×55 | W14×342 | | 4 | 37.1 | 1.41 | W18×55 | W14×283 |
| | 3 | 40.3 | 1.42 | W16×45 | W14×342 | | 3 | 41.9 | 1.41 | W16×45 | W14×283 |
| | 2 | 41.9 | 1.42 | W18×55 | W14×426 | | 2 | 41.9 | 1.41 | W18×55 | W14×370 |
| | 1 | 45.2 | 1.42 | W18×97 | W14×426 | | 1 | 46.8 | 1.41 | W18×97 | W14×370 |

(1)    area of brace steel core

## 3.  Seismic Performance Assessment

3.1 Modeling

For the linear analysis procedures, the buildings are modeled as described in the previous design section. For the nonlinear analysis procedures, the buildings are modeled in three dimensions using PERFORM-3D [12]. The modeling approach is similar to that used for the linear analysis procedures except that nonlinear elements are utilized. The BRBF beams and columns are modeled with nonlinear compound components to capture any nonlinear demands. Plastic hinges are placed in the beam just outside the brace-intersection and in the column above and below each beam-to-column connection. The BRBs are modeled using single compound elements connecting working points. These compound elements consist of an inelastic portion and an elastic portion. The inelastic portion is given properties consistent with the BRB steel core. The elastic portion is given an area such that the compound component achieves an overall stiffness equal to $KF \times A_{sc} \times E / L_{w.p.}$. The PERFORM-3D endzone feature for the BRB component is not used.

The BRB axial force-deformation behavior is modeled following guidelines given by Burkett and Lopez [13]. Table 2 summarizes the parameters adopted and Fig. 2(a) shows the generalized force-deformation curve that defines some of the variables. Plastic deformation parameters, (*a*, *b* and, *c* – not shown in the table or

figure), are taken directly from ASCE 41 Table 9-7, except no strength loss is captured due to the limitations in the PERFORM-3D BRB component. The nonlinear force-deformation model follows an asymmetric trilinear curve in tension and in compression. The adequacy of the model is qualitatively validated (i.e, by visual inspection) with test data as shown in Fig. 2 (b).

## 3.2 Hazard and Performance Level

The seismic hazard used for the performance assessment is the same as that used in the design. For the linear assessments, the forces are derived using the risk-targeted maximum considered earthquake ($MCE_R$) spectrum defined in ASCE 7. For the nonlinear static assessment, the $MCE_R$ is similarly used to derive the target displacement value. For the nonlinear dynamic assessment, the $MCE_R$ is used as the target spectrum for selecting and scaling the ground motions. The ground motions are selected from a suite of 44 records used in FEMA P695 [14]. Fourteen records with the least error (measured by computing the absolute area between the target spectrum and the individual spectrum over a structural period range of $0.2T_1$ to $1.5T_1$) are selected for the nonlinear analysis, but with no two records coming from the same station. The structural assessment is conducted using the collapse prevention (CP) performance level, which is the typical level considered when using an MCE-level hazard.

## 3.2 Analysis Details

The nonlinear analysis is set to terminate when the solution fails to converge or when an arbitrary roof drift ratio of 20 percent is reached. Though convergence limits and drift limits are often used as an indicator of collapse, in this study collapse is evaluated by using the assessment criteria alone (via allowable component limits in ASCE 41 Table 9-4 and Table 9-7). Collapse modes not explicitly modeled herein (e.g., failures in the gravity framing system) would likely occur well before 20 percent is reached.

Table 2 – Inelastic component properties used in PERFORM-3D model calibration

| Variable | K0 | KF | FY | FU0 | FUH(tension) | FUH(compression) | DU | DX |
|----------|-----|-----|-----|-----|--------------|------------------|-----|-----|
| Value | $K_{sc}$ | $0.02K_{EFF}$[1] | $0.89P_{y,sc}$[2] | $1.05P_{y,sc}$[3] | $1.34P_{y,sc}$ | $1.51P_{y,sc}$ | $0.0058L_{yz}$[4] | $0.04L_{yz}$ |

(1) $K_{sc}$ = brace core stiffness (2) $K_{EFF}$ = brace overall elastic stiffness (3) $P_{y,sc}$ = yield strength of steel core, $A_{sc}F_y$ (4) $L_{yz}$ = length of the yield zone
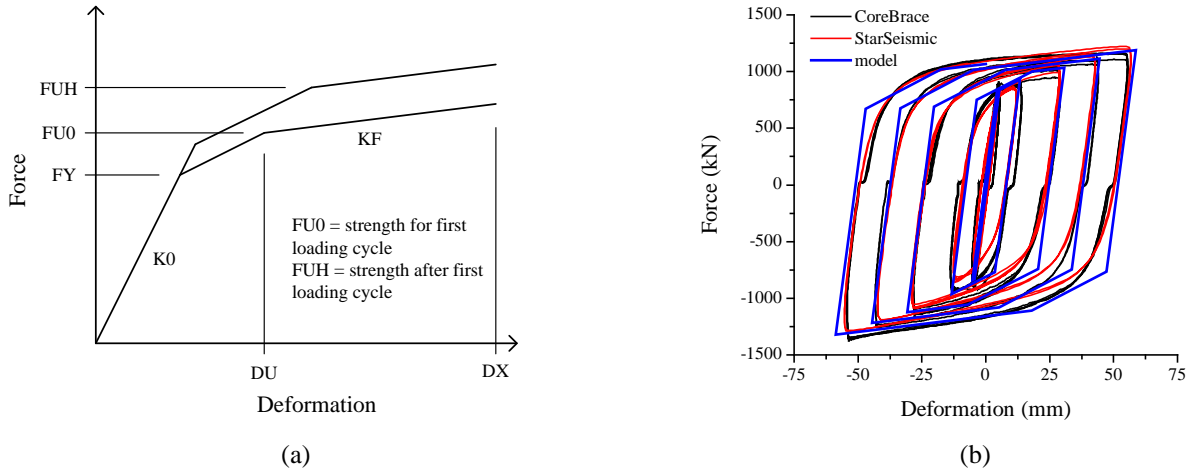
(a)



(b)

Fig. 2 – (a) Generic force-deformation plot showing the BRB inelastic component model property definitions in PERFORM-3D and (b) force-deformation response of BRB inelastic portion assuming $L_{yz}$ = 3.3 m (130 in.) and $A_{sc}$ = 29 mm$^2$ (4.5 in$^2$). The experimental data is converted from data reported for a StarSeismic BRB in Merritt, Uang [15] and a CoreBrace BRB in Newell, Uang [16].

# 4. Seismic Assessment Results

## 4.1 Results Format

The results are presented in terms of a normalized demand-capacity ratio, $DCR_N$. If the value is less than unity, the component satisfies the acceptance criteria for the given hazard / performance level combination. This $DCR_N$ is not to be confused with the $DCR$ defined in ASCE 41 §7.3, which is the demand-capacity ratio considering unreduced earthquake forces. For the linear analysis, $DCR_N$ is defined in Eq. (1) and Eq. (2):

$$\text{Deformation-controlled:} \quad DCR_N = \frac{Q_{UD}}{m\kappa Q_{CE}} \tag{1}$$

$$\text{Force-controlled:} \quad DCR_N = \frac{Q_{UF}}{\kappa Q_{CL}} \tag{2}$$

where $Q_{UD}$ is the deformation-controlled demand, $Q_{UF}$ is the force-controlled demand, $Q_{CE}$ is the expected strength, $Q_{CL}$ is the lower-bound strength, $m$ is the component demand modification factor, and $\kappa$ is the knowledge factor (taken as unity in this study).

For the nonlinear analysis results, $DCR_N$ is defined in Eq. (3) and Eq. (4):

$$\text{Deformation-controlled:} \quad DCR_N = \frac{Q_{UD}}{\kappa Q_{CE}} = \begin{cases} Total & \dfrac{\theta_{plastic} + \theta_{elastic}}{\kappa\left(\theta_y + \theta_{pe} + \theta_{p,AC}\right)} \\[3mm] Plastic & \dfrac{\theta_{plastic}}{\kappa\theta_{p,AC}} \end{cases} \tag{3}$$

$$\text{Force-controlled:} \quad DCR_N = \frac{Q_{UF}}{\kappa Q_{CL}} \text{ and } DCR_N = \frac{\theta_{total}}{\kappa\theta_y} \tag{4}$$

where $\theta_{plastic}$ is the plastic deformation, $\theta_{elastic}$ is the elastic deformation, $\theta_y$ is the expected yield deformation, $\theta_{pe}$ is the post-yield elastic deformation, $\theta_{total}$ is the total deformation, and $\theta_{p,AC}$ is the acceptance criterion based on plastic deformation.

For steel components in ASCE 41, inelastic deformation parameters are provided in terms of plastic deformations rather than total deformations. The choice of whether to use plastic deformations or total deformations will depend on what nonlinear component model is adopted for each component action (e.g., moment-curvature hinge or moment-rotation hinge). Consequently, yield and post-yield elastic deformations may need to be added to the values given in ASCE 41 to determine the total deformation for each structural performance metric. For the axial deformation in the BRBs, PERFORM-3D outputs the results in terms of total deformations and these total deformations are used directly in the assessment.

Once the $DCR_N$ values are obtained, they are presented together on one plot for all four analysis procedures. This is done to easily compare the results, though it should be noted that linear and nonlinear $DCR_N$ values are arrived at in a fundamentally different way (e.g., linear is calculated based on forces vs. nonlinear is calculated based on deformations).

## 4.2 Results and Discussion

The brace results for the 4-, 8-, and 16-story ELF-designed frames are presented in Fig. 3, Fig. 5, and Fig. 7, respectively. The brace results for the 4-, 8-, and 16-story RSA-designed frames are presented in Fig. 4, Fig. 6, and Fig. 8, respectively. In the figures, L is for Left and R is for Right. All four analysis procedures are represented in the graphs. Three of the results (i.e., lines) are labeled as LSP for the linear static procedure, LDP for the linear dynamic procedure, and NSP for the nonlinear static procedure. The results from the nonlinear dynamic procedure (NDP) are reported using the median, mean, 84th percentile, and mean plus one standard deviation for the ground motion set.

For the 4-story frames, the results generally indicate acceptable performance of the BRBs. The linear procedures tend to be more conservative than the nonlinear procedures. The linear static procedure indicates some of the braces fail the collapse prevention criteria for the ELF-designed frame and all of the braces fail the CP criteria for the RSA-designed frame. However, the maximum $DCR_N$ value is approximately 1.2, which may not be too concerning given the inherent uncertainty in the assessment. The nonlinear procedures indicate that the BRBs do not experience deformations greater than the allowable, with the dispersion of results (84th percentile and the mean + std.) showing a reasonably tight distribution that suggests that none of the frames lose stability.

For the 8-story frames, the results are noticeably different than those seen in the 4-story frames. The linear procedures tend to be less conservative than the nonlinear dynamic procedure, which is not expected. For the ELF-designed frame, the linear procedures show the braces passing the assessment. For the RSA-designed frame, the LDP indicates acceptable performance but the LSP indicates failure. This is not surprising given the contrast in the lateral load distributions used in the RSA design and the LSP assessment.

In contrast to the linear procedures, the nonlinear dynamic procedure suggests the worst performance. Both the ELF-designed frame and the RSA-designed frame have brace problems at the mid-height of the building. The problem is more pronounced for the RSA-designed frame, which can again be explained by the reduced member capacities resulting from the design force distribution. The mean and median values are reasonably close together, suggesting there is limited large inelastic demand excursions. The dispersion in demand is largest for the first story brace in the RSA-designed frame, suggesting that the building reaches a point of instability. This highlights how the mean value may not be a good measure of the brace performance, especially for this first story result. The inherent assumption in the mean value presented is that the $DCR_N$ values are distributed normally. However, when a frame goes highly nonlinear and reaches large drift levels, the results may be better represented by a lognormal distribution [17]. Therefore, the median or the mean (calculated assuming a lognormal distribution) are more significant.

For the 16-story frames, the results indicate better performance than seen in the 8-story frames and are more in line with those seen in the 4-story frames. For the 16-story ELF-designed frame, the linear procedures

indicate the braces pass the assessment criteria; maximum $DCR_N$ values are around 0.8. Though not previously discussed, the *design* demand-capacity ratios are in the 0.8-0.9 range, thus the values given by the assessment methodology are less conservative (i.e., lower) for this case. This is partly due to the difference in how ASCE 7 and ASCE 41 determine the period used in the force calculations. ASCE 7 requires the period not be greater than an upper-bound (i.e., $C_uT_a$), and ASCE 41 allows the period computed in analysis to be used directly. This can have a significant effect on the forces applied to the system.

For the 16-story RSA-designed frame, the linear static procedure pushes some of the mid-height braces beyond their allowable deformations. Given the contrast in the design and assessment force distributions for this case, failure of these mid-height braces is not surprising. Nevertheless, the maximum $DCR_N$ values are around 1.1, which suggest little change would need to be made to the design to pass the assessment.
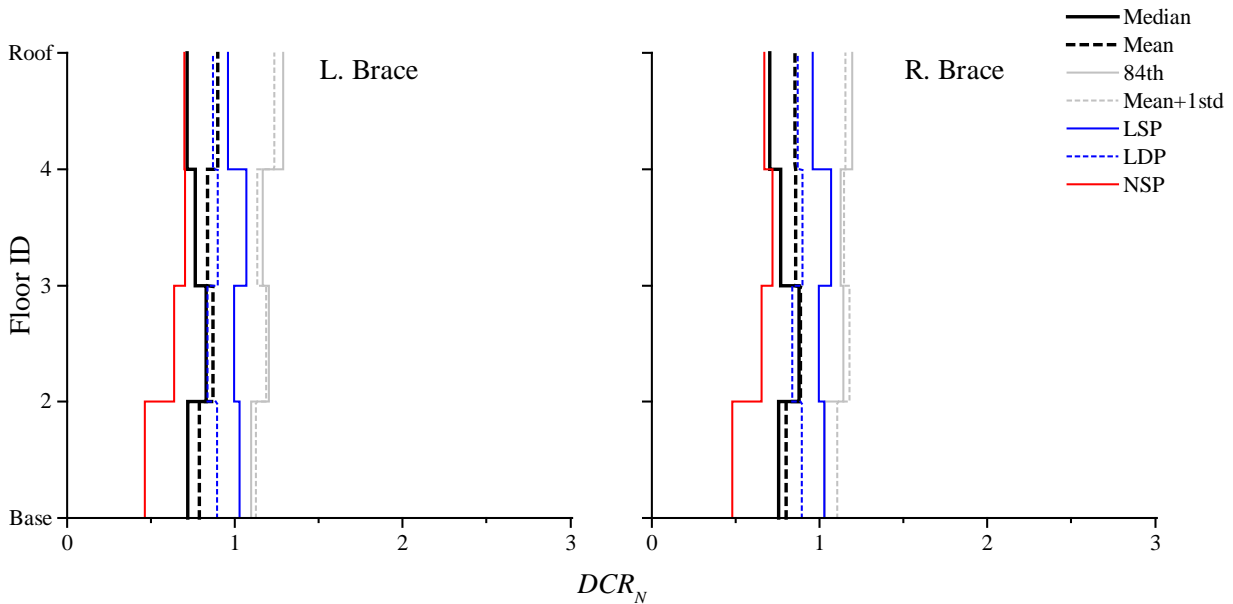


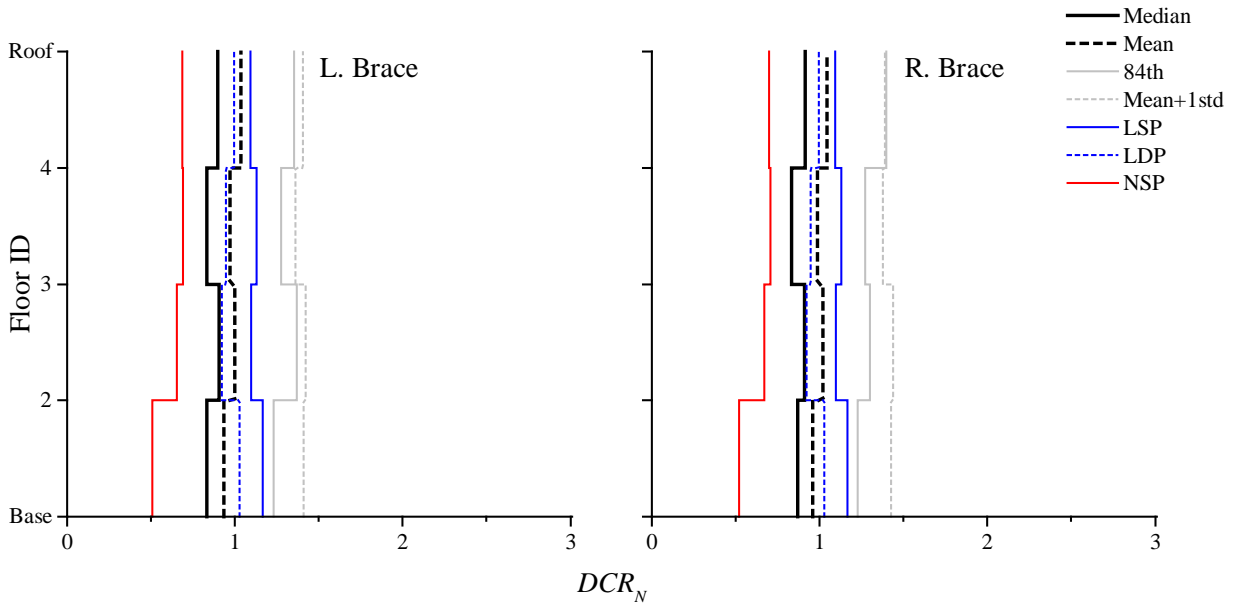Fig. 3 – Results for the 4-story ELF-designed frame (considering CP at $MCE_R$)

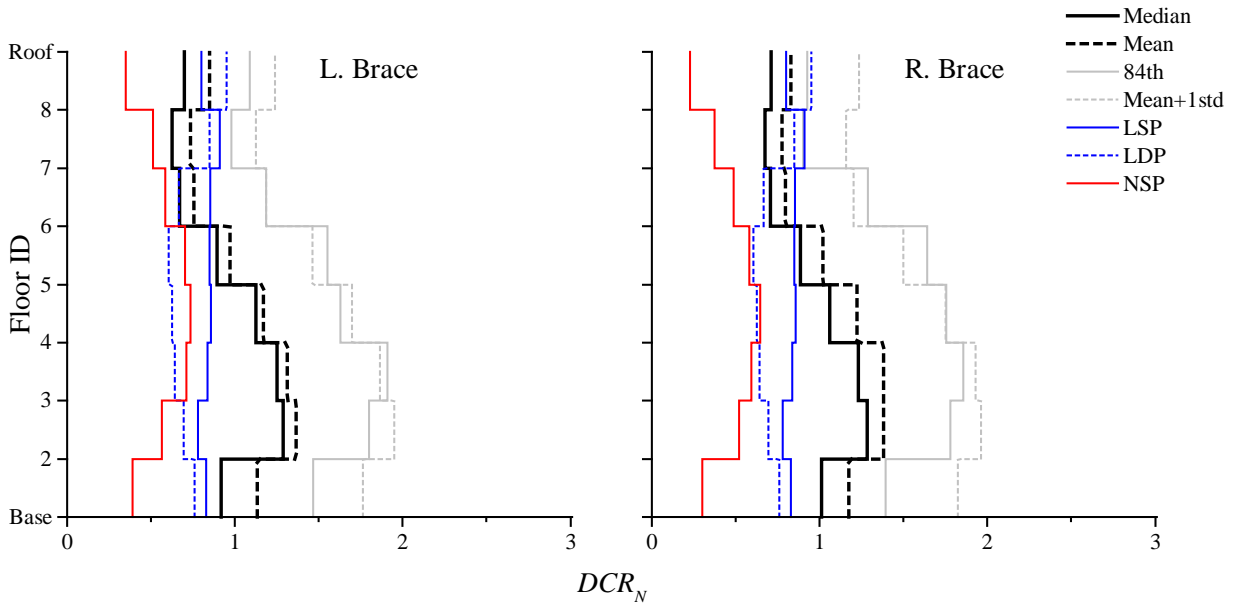Fig. 4 – Results for the 4-story RSA-designed frame (considering CP at $MCE_R$)



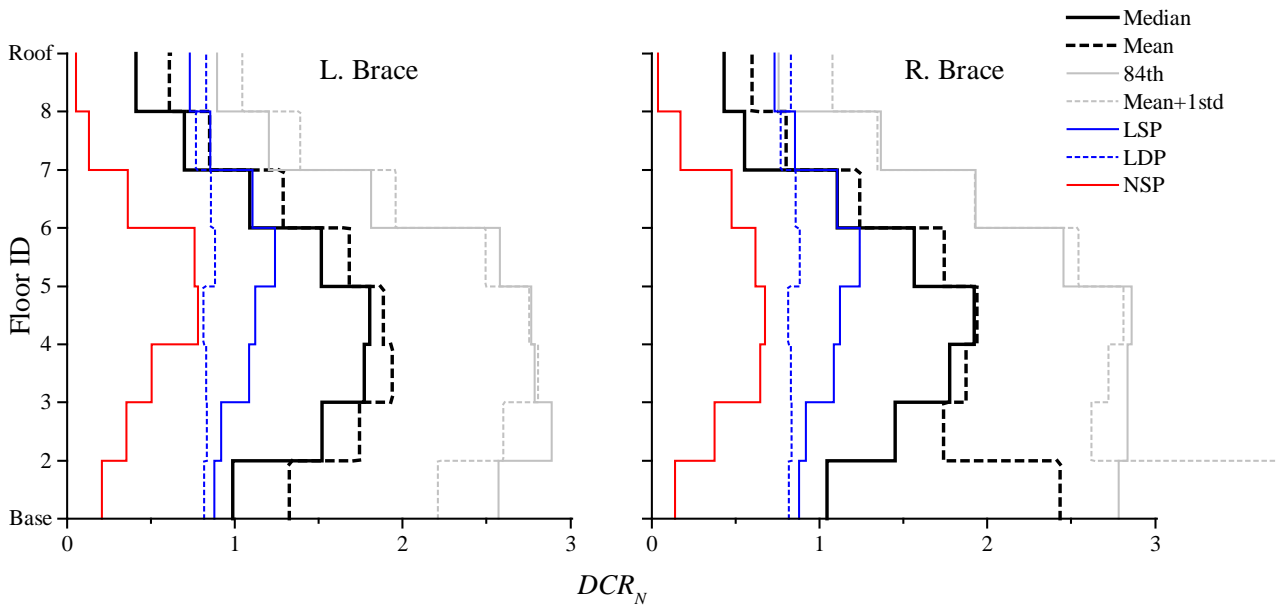Fig. 5 – Results for the 8-story ELF-designed frame (considering CP at $MCE_R$)

Fig. 6 – Results for the 8-story RSA-designed frame (considering CP at $MCE_R$)

The nonlinear dynamic results for the 16-story frames take on different deformation patterns as compared to the linear results, though the median $DCR_N$ value stays below unity in all of the braces. In the ELF-designed frame, the highest demands are in the lower and upper stories, which highlights the influence of higher mode effects. Higher modes are not accounted for in the ELF design force distribution. However, the ELF-designed frame has sufficient capacity to pass the collapse prevention assessment criteria. It also passes the nonlinear static assessment.

In contrast to the ELF-designed frame, the RSA-designed frame has a more uniform distribution of peak demands over its height. This suggests that the RSA-designed frame's design force distribution is more in line with the nonlinear demands from the earthquake suite. The dispersion of $DCR_N$ value is also higher for the RSA-designed frame, especially in the story range of maximum demands. This dispersion indicates that there are several ground motions records that are pushing the frame to large drift levels.
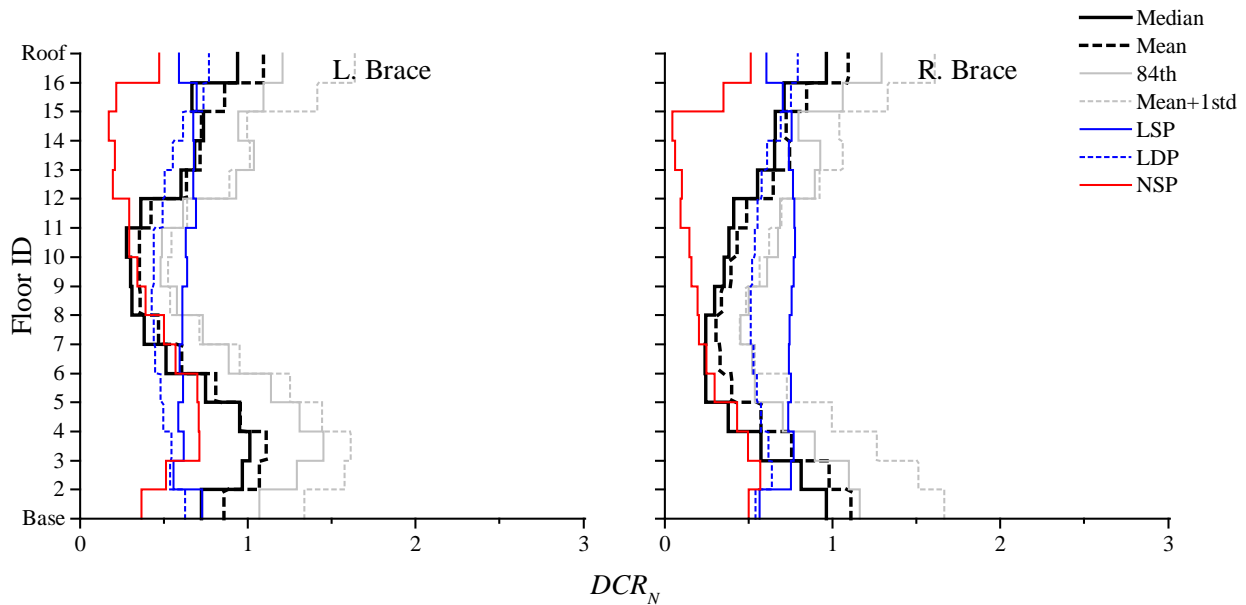
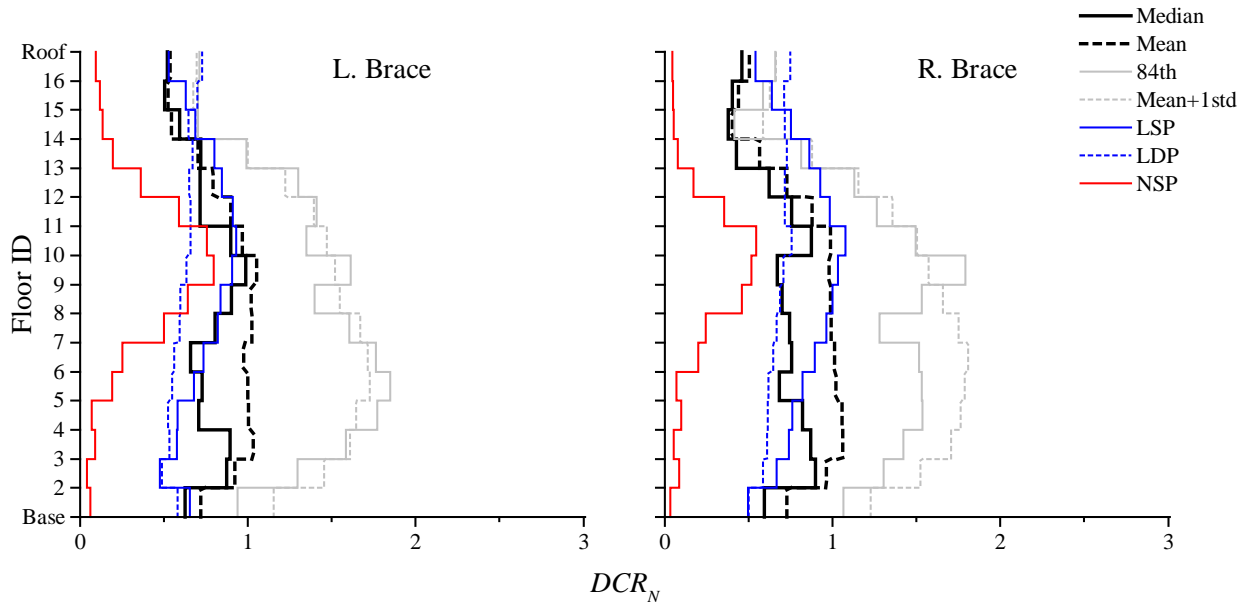Fig. 7 – Results for the 16-story ELF-designed frame (considering CP at BSE-2)



Fig. 8 – Results for the 16-story RSA-designed frame (considering CP at BSE-2)

## 4. Conclusions

This paper investigates the ASCE 41 predicted seismic performance of a suite of buckling-restrained braced frames designed with ASCE 7 in order to compare the consistency of the two standards. The linear and nonlinear results generally indicate acceptable performance for the buckling-restrained braces when subjected to a risk-targeted maximum considered earthquake and assessed with the collapse prevention performance level, except for the 8-story frames. The braces in the 8-story frames failed the assessment criteria for both the linear and nonlinear procedures, which highlights the challenges of capturing the nonlinear response of a building with linear design procedures. Interestingly, the ELF-designed frames generally performed better than the RSA-

designed frames. Amongst the four assessment procedures employed, a variety of performance outcomes were reached. The linear results are not always more conservative than the nonlinear results, which is counterintuitive and could discourage use of ASCE 41 in new building design or the retrofit of an existing building. Additionally, the nonlinear static procedure always indicated satisfactory performance, which is typically thought to be more conservative than the nonlinear dynamic procedure. Though all the components of the BRBF were not assessed in this paper (e.g., beams and columns), the results herein give the engineer examples of how the braces of a BRBF will perform, as indicated by an ASCE 41 assessment, for three different heights and two different design approaches. Ultimately, the results from this study would need to be compared with the results provided from analyzing the buildings in a FEMA P695 analysis. This comparison would provide the supplementary information needed to correlate the two standards. However, ASCE 41 has not yet moved to a risk-based philosophy aligned with ASCE 7.

## 4. Disclaimer

Certain commercial software may have been used in the preparation of information contributing to this paper. Identification in this paper is not intended to imply recommendation or endorsement by NIST, nor is it intended to imply that such software is necessarily the best available for the purpose. Mean, median, and associated variances are reported for the nonlinear dynamic results, which illustrates some of the uncertainty inherent in the selection process for input ground motions. Beyond this important issue, no formal investigation of uncertainty or error is included in this study. The question of uncertainty in the analytical models, solution algorithms, and material properties are beyond the scope of the work reported here.

## 5. References

[1] ICC (2012): *International Building Code (IBC)*. Washington, DC: International Code Council.
[2] ASCE (2010): *Minimum Design Loads for Buildings and Other Structures*, in *ASCE/SEI 7-10*, American Society of Civil Engineers: Reston, VA.
[3] ASCE (2013): *Seismic Evaluation and Retrofit of Existing Buildings*, in *ASCE/SEI 41-13*, American Society of Civil Engineers: Reston, VA.
[4] Harris JL, Speicher MS (2015): *Assessment of First Generation Performance-Based Seismic Design Methods for New Steel Buildings Volume 2: Special Concentrically Braced Frames*, National Institute of Standards and Technology: Gaithersburg, MD.
[5] Speicher MS, Harris III JL (2016): Collapse prevention seismic performance assessment of new special concentrically braced frames using ASCE 41. *Engineering Structures*. 126: p. 652-666.
[6] Speicher MS, Harris III JL (2016): Collapse Prevention Seismic Performance Assessment of New Eccentrically Braced Frames using ASCE 41. *Engineering Structures*. 117: p. 344-357.
[7] Harris JL, Speicher MS (2015): *Assessment of First Generation Performance-Based Seismic Design Methods for New Steel Buildings Volume 3: Eccentrically Braced Frames*, National Institute of Standards and Technology: Gaithersburg, MD.
[8] Harris JL, Speicher MS (2015): *Assessment of First Generation Performance-Based Seismic Design Methods for New Steel Buildings Volume 1: Special Moment Frames*, National Institute of Standards and Technology: Gaithersburg, MD.
[9] AISC (2010): *Specification for Structural Steel Buildings*, in *ANSI/AISC 360-10*, American Institute of Steel Construction: Chicago, IL.
[10] AISC (2010): *Seismic Provisions for Structural Steel Buildings*, in *ANSI/AISC 341-10*, American Institute of Steel Construction: Chicago, IL.
[11] CSI (2013): *Extended Three Dimensional Analysis of Building Systems*, in *ETABS*, Computers and Structures, Inc.: Berkeley, CA.
[12] CSI (2013): *Nonlinear Analysis and Performance Assessment for 3D Structures*, in *PERFORM 3D*, Computers and Structures, Inc.: Berkeley, CA.
[13] Burkett L, Lopez W (2011): *Perform Nonlinear Component Modeling of StarSeismic' Powercat$^{TM}$ BRBs*.
[14] FEMA (2009): *Quantification of Building Seismic Performance Factors*, in *FEMA P695*, Department of Homeland Security: Washington, D.C.
[15] Merritt S, Uang C-M, Benzoni G (2003): *Subassemblage Testing of Star Seismic Buckling-Restrained Braces*, University of California, San Diego.

[16] Newell J, Uang C-M, Benzoni G (2006): *Subassemblage Testing of CoreBrace Buckling-Restrained Braces (G Series)*, University of California, San Diego.

[17] Uribe R, Sattar S, Speicher MS, Ibarra L  (2017): Influence of Ground Motion Selection on the Assessment of a Steel Special Moment Frame. in *16th World Conference on Earthquake Engineering, 16WCEE 2017*. Santiago, Chile.